Heterogeneous Catalysis

DOI: 10.1002/anie.201203282

Kinetics of the Fischer–Tropsch Reaction**

Albert J. Markvoort, Rutger A. van Santen, Peter A. J. Hilbers, and Emiel J. M. Hensen*

The Fischer–Tropsch (FT) reaction is a heterogeneous catalytic reaction that converts synthesis gas, that is, a mixture of carbon monoxide (CO) and hydrogen (H_2), into mainly linear hydrocarbons. Fundamental interest in this reaction[1] has been renewed because of its use in the conversion of natural gas, coal, and biomass into liquid fuels.[2] The reaction is initiated by dissociative adsorption of CO at the catalyst surface. Adsorbed hydrogenated single carbon atom CH_x intermediates self-organize into adsorbed linear hydrocarbon chains, which desorb from the surface as alkanes or alkenes by reaction with hydrogen atoms or as aldehydes or alcohols by insertion of CO.[3–6] A persisting challenge is the design of a catalyst that maximizes the production of long-chain hydrocarbons while limiting the formation of undesired methane.

Recent important insights in the influence of specific catalytic surface sites on the individual reaction steps, obtained from many computational (mainly DFT-based quantum-chemical) studies,[7–12] are that the rates of CO dissociation and C–C bond formation[13] are highly dependent on the structure of the catalyst surface, and that the chain growth reaction is reversible.[12,14] The latter contradicts the generally accepted view that the chain growth consists of a sequence of irreversible reaction steps,[2] an assumption which provides a basis for widely used kinetic models of this reaction.[15,16] In addition, a major advance in computational catalysis has been the formulation of a theoretical framework that enables to predict the activity of a catalytic reaction from the relative (free) energies of reaction intermediates and their corresponding elementary rate constants. Competition between reagent activation and product formation leads to a volcano-type dependence of the reaction rate on the reactivity of the catalyst surface, called the Sabatier principle.[17] An important question is whether such a general framework also exists for the selectivity of the Fischer–Tropsch reaction.

Here we present, inspired by our recent models for dynamic supramolecular (co)polymerizations,[18] a kinetic model that takes into account the full reversibility of the chain growth to analyze the kinetic parameter relations that actually control the selectivity and activity of the Fischer–Tropsch (FT) process. Trends in the reactivity as a function of the relative stability of the reaction intermediates and the positions of catalytically reactive metal in the periodic system are indicated. It is shown that on a Langmuir surface, where all adsorption sites have an equal affinity for the adsorbing species, the high chain growth condition does not coincide with a high conversion, as the surface becomes poisoned by growing hydrocarbon chains. Finally, based on previously published quantum-chemical results,[19] a dual reaction center model is proposed that is shown to have substantially higher chain growth at high CO conversion.

Our model, which is based on the currently generally accepted carbide mechanism for the formation of hydrocarbons by the FT reaction,[6] is schematically depicted in Figure 1 a, whereas Figure 1 b shows different catalyst states.

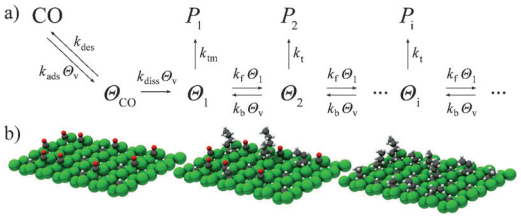

Figure 1. Fischer–Tropsch model for single reaction centers. a) The reaction steps, their rate constants, and their dependencies on reactants, where Θ_{CO} represents adsorbed CO, Θ_i adsorbed chains of i carbon atoms, Θ_v vacant surface sites, and P_i desorbed alkanes of length i. b) Different states of the catalyst surface. On the right side: Surface with adsorbed CO and CH_x only. In the middle: Hydrocarbon chain growth accompanied with CO adsorption/dissociation. On the left side: A surface poisoned with growing carbon chains.

In the model, we do not consider hydrogen transfer steps explicitly, but include them and other reaction steps with the rate parameters for the carbon species. CO adsorbs to and desorbs from vacant surface sites with rate constants k_{ads} and k_{des}, where adsorbed hydrogen atoms are considered not to affect chemisorption.[20] Adsorbed CO can dissociate, with a rate constant k_{diss}, to give C_1, where we do not distinguish between hydrogen-assisted or direct CO dissociation and include the formation of adsorbed CH_x in one reaction step, such that also only one type of CH_x monomer is considered. Removal of O_{ads} from the surface is considered to be fast. All chain growth reaction steps, converting a C_i chain plus a C_1 into a C_{i+1}, are considered to being reversible with rate constants k_f and k_b, which are independent of the chain length.

[*] Dr. A. J. Markvoort, Prof. Dr. P. A. J. Hilbers
Institute for Complex Molecular Systems
Department of Biomedical Engineering
Eindhoven University of Technology
PO Box 513, 5600 MB, Eindhoven (The Netherlands)
E-mail: a.j.markvoort@tue.nl
Prof. Dr. R. A. van Santen, Prof. Dr. E. J. M. Hensen
Institute for Complex Molecular Systems
Eindhoven University of Technology
PO Box 513, 5600 MB, Eindhoven (The Netherlands)

[**] We thank Mark Peletier and Huub ten Eikelder for useful discussions on the mathematics of reversible chain growth partial differential equations.

Supporting information for this article is available on the WWW under http://dx.doi.org/10.1002/anie.201203282.

Finally, C_1 desorbs as methane with a rate constant k_{tm}, whereas chains C_i with $i \geq 2$ (C_{2+}) adsorb with a rate constant k_t, which is independent of the chain length. Readsorption of product molecules is not considered.

The surface consists of catalytic sites that can either be vacant or occupied by an adsorbed CO molecule, a C_1, or a carbon chain with $i \geq 2$. These occupying molecules are described by concentrations Θ_v, Θ_{CO}, Θ_1, and Θ_i, respectively, with the constraint $\Theta_{CO} + \Theta_v + \Sigma_i \Theta_i = 1$. The kinetics of the model is described by the standard rate equations corresponding to the reactions in Figure 1 a, while the steady state can also be calculated using a mass balance approach (see the Supporting Information for details).

Since the rate constants are chain-length independent (for $i \geq 2$), the ratio $\alpha = \Theta_{i+1}/\Theta_i$ is chain-length independent and given by the quadratic Equation (1),

$$k_f\Theta_1 - (k_f\Theta_1 + k_b\Theta_v + k_t)\alpha + k_b\Theta_v\alpha^2 = 0 \quad (1)$$

where only one of the two square roots is physically meaningful, that is, between 0 and 1, keeping the total mass finite. The product distribution ($i > 1$) will thus reflect the characteristic logarithmic Schultz–Anderson–Flory dependence on the chain length, which is often found experimentally.[3,15] Interestingly, the analogous formula for $\alpha_1 = \Theta_2/\Theta_1$ shows that this ratio is, even when $k_{tm} \neq k_t$, also equal to α. Because of the chain-length independent α, $\Sigma_i\Theta_i = \Theta_1/(1-\alpha)$, and the CO conversion and selectivity for methane are given by Equation (2)

$$r_{CO} = \left(k_{tm} - k_t + \frac{k_t}{(1-\alpha)^2}\right)\Theta_1 \quad (2)$$

and Equation (3),

$$Sel_{CH_4} = \frac{\frac{d}{dt}[CH_4]}{-\frac{d}{dt}[CO]} = \frac{k_m}{k_m - k_t + k_t/(1-\alpha)^2} \quad (3)$$

respectively.

First we study the dependence on individual rate constants (k_{des}, k_{diss}, k_f, k_b, and k_t) by varying one rate constant a time, for the case $k_{tm} = k_t$. Figure 2 a shows the k_b dependence of the chain growth rate α, the rate of the conversion of CO , and the surface coverage for three values of k_t. We observe the expected decrease in α upon an increased termination rate. Then the rate of product formation becomes so high that chains no longer get the chance to grow and the decrease in the concentration of growing chains increases the concentration of the surface vacancies. One observes that α is not affected by k_b until k_b/k_f equals one and only starts to decline steeply when this ratio exceeds ten. This is important as it appears from DFT calculations that the ratio k_b/k_f may strongly depend on the surface structure and the metal,[10,11,14,21] and the classical expression $\alpha = k_f\Theta_1/(k_f\Theta_1 + k_t)$ can thus only be used if $k_b/k_f < 10$.

Figure 2 b shows performance parameters α and r_{CO}, and surface concentrations as a function of k_{diss} for various values of $k_f = k_b$. The solid lines represent the case without chain growth where only methane is produced. We recognize three different k_{diss}/k_t regimes. For low dissociation, $k_{diss}/k_t < 1$, termination is fast compared to C_1 formation, resulting in a low concentration of C_1 as well as a small α, but high CO coverage. In the second regime, $1 < k_{diss}/k_t < 10$, CO on the surface becomes gradually displaced by growing hydrocarbon chains. CO dissociation remains rate controlling, resulting in an intermediate value of α. In the third regime, $k_{diss}/k_t > 10$, k_t is rate controlling, α is high, and the CO coverage is low.

Figure 2 c shows the steady-state production, surface coverage, and reference CO concentration (Θ_{CO}^{ref}) as a function of the CO surface coverage, where $\Theta_{CO}^{ref} = k_{ads}\cdot P_{CO}/(k_{ads}\cdot P_{CO} + k_{des})$ would be the CO coverage in absence of CO dissociation and where CO coverage is changed by varying the rate of CO desorption. The bottom part of Figure 2 c shows that, starting from a low desorption rate, that is, $\Theta_{CO}^{ref} \approx 1$, the surface concentration of CO decreases much stronger than the reference CO coverage. As also observed experimentally,[22] the surface becomes initially covered with C_1 species that replace CO. At lower coverage CO is replaced increasingly by growing hydrocarbon chains, covering a large extend of the surface. The coverage of C_1 gradually increases with decreasing Θ_{CO} as for high desorption rates the surface finally becomes almost empty. Also the CO conversion and α show a maximum as a function of the CO coverage. Although α is almost constant over a large range, it vanishes when the CO coverage is either low or close to one. At high CO coverage the surface becomes nonreactive as there are

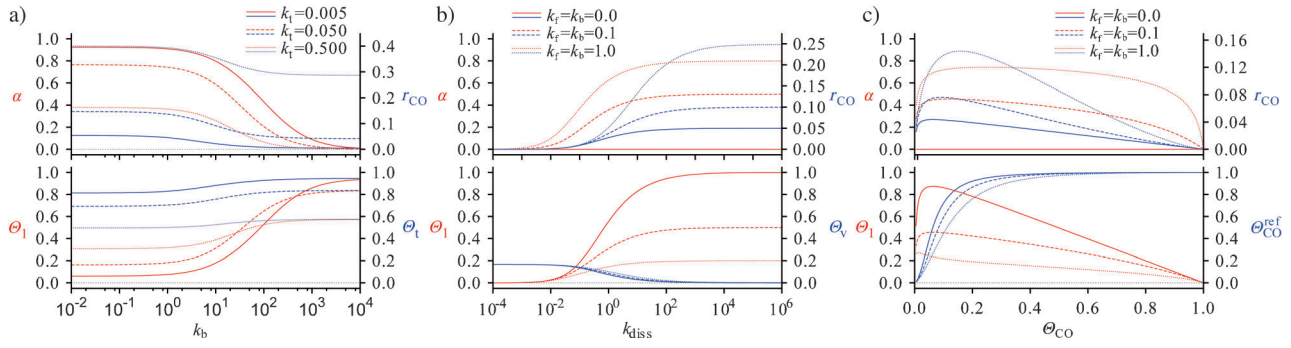

Figure 2. Dependence of the steady-state production (r_{CO}), chain-growth rate α, and surface coverage on the rate constants. a) As a function of k_b for three values of k_t. b) As a function of k_{diss} for three values of $k_b = k_f$. c) As a function of Θ_{CO} (by varying k_{des}) for three values of $k_b = k_f$. Values of not mentioned rate constants are $k_{ads}\,P_{CO} = 100$, $k_{des} = 20$, $k_{diss} = 11$, $k_b = k_f = 1$, and $k_t = 0.05$.

hardly any surface sites available for chain growth, whereas at low Θ_{CO} the surface becomes nonreactive as it is completely covered by growing chains.

From the above-mentioned results we conclude that a high chain growth (α) can be obtained when k_b does not exceed k_f, k_{diss} is large compared to k_{tm}, and k_f is large compared to k_t. However, we also notice conflicting conditions for a high conversion and high α, because a high conversion requires sufficient CO on the surface which should thus not be poisoned by growing hydrocarbon chains. Moreover, the different rate constants cannot be varied individually, as all are a function of the surface reactivity,[17] that is identified with adsorption energies of C_{ads} and O_{ads}. The reactivity increases from right to left as for the metals in a row of the periodic system.[23] A well-developed procedure in computational catalysis uses Brønsted–Evans–Polanyi linear activation–reaction energy relations to relate activation energies of surface reactions with changes in the adsorption energies of the surface adatoms or reaction intermediates. Thus, the four controlling rate constants, k_{diss}, k_t, k_f, and k_b, are correlated. Extensive literature exists on the selection of the Brønsted–Evans–Polanyi proportionality constants.[13,17,24]

To illustrate the effect of the performance-controlling rate parameter relation of the catalyst, Figure 3 shows the resulting dependence of α and CO conversion on the surface reactivity, where also the positions of different metals are indicated schematically.

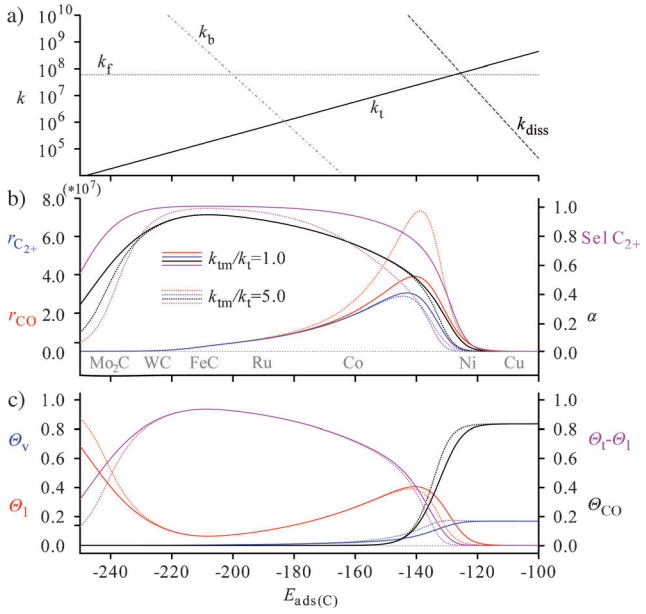

Figure 3. Performance of the catalyst as a function of the surface reactivity. a) Brønsted–Evans–Polanyi relations $k_x = A_x \exp\left[-\left(E_x^0 + \beta_x E_{ads(C)}\right)/RT\right]$ are used to relate rate constants to the surface reactivity ($E_{ads(C)}$), at temperature $T = 500$ K and parameters $A_t = 10^{17}\ s^{-1}$, $\beta_t = -0.30$, and $E_t^0 = 50\ kJ\,mol^{-1}$ for a termination rate k_t, $A_{diss} = 10^{13}\ s^{-1}$, $\beta_{diss} = 1.2$, and $E_{diss}{}^0 = 200\ kJ\,mol^{-1}$ for a CO dissociation rate k_{diss}, $A_f = 10^{13}\ s^{-1}$, $\beta_f = 0.0$, and $E_f^0 = 50\ kJ\,mol^{-1}$ for a chain growth rate k_f, and $A_b = 10^{13}\ s^{-1}$, $\beta_b = 1.0$, and $E_b^0 = 250\ kJ\,mol^{-1}$ for a bond cleavage rate k_b. b) Total CO conversion (r_{CO}), production of carbon chains C_{2+} ($r_{C_{2+}}$), chain growth factor α, and selectivity for C_{2+} production (Sel C_{2+}). c) Surface coverage, where $\Theta_t = \sum_{i=1}^{\infty} \Theta_i$; $C_{2+} = C_i$ with $i \geq 2$.

Starting at the right-hand side, one observes catalysts with low carbon adsorption energy to be either inactive (Cu) or to form exclusively methane (Ni). When the surface reactivity increases from a low reactivity surface, at which hardly any CO dissociates but CH_x intermediates are rapidly hydrogenated, to a surface that can dissociate CO with a slightly decreased rate for the CH_x hydrogenation, α and the conversion of CO increase. Next to CO also intermediate CH_x appears on the surface. When the surface reactivity increases further, the rate of the chain termination is controlling and a high chain-growth parameter α is found. For a high surface reactivity the reverse reaction of C–C bond cleavage becomes fast and the chain-growth selectivity decreases. The trend in methane selectivity agrees surprisingly well with experimental observations.[6] The optimum rate of the CO conversion is related to the initial decrease in the CO coverage and the increase in the C_1 concentration. The decrease in CO conversion to the left relates to the increasing coverage with growing hydrocarbon chains.

Approximate expressions can be derived for the operationally relevant case where CO dissociation is not rate controlling and α is high [Eq. (4)]:

$$\alpha = \left(1 + \sqrt{\frac{k_t}{k_f(1-\Theta_{CO})}}\right)^{-1}$$
$$r_{CO} = (k_{tm} - k_t)\sqrt{\frac{k_t}{k_f}}(1-\Theta_{CO})^{1/2} + \sqrt{k_t k_f}(1-\Theta_{CO})^{3/2} \quad (4)$$

with Equation (5).

$$\Theta_{CO} \approx \left[\frac{K_{eq}^{CO} P_{CO}}{k_{diss}}\right]^{1/2} (k_f k_t)^{1/4}. \quad (5)$$

These expressions show that for such high values of α the rate of CO conversion is suppressed with increasing CO pressure, which is due to poisoning of the catalyst with growing chains.

A two center site with one center for CO dissociation and one for chain growth could prevent such poisoning. Recent quantum-chemical calculations indicate the possibility of such a site,[19] which is not to be confused with, though this idea is also not opposing, the idea of multiple types of independently operating sites on a working catalyst.[25] Extension (see Figure 4a) of the model to incorporate this feature indeed shows a substantial improvement in the consumption rate for a highly selective production of C_{2+} (Figure 4b). The essential expression that changes for the dual reaction center model is that for the surface coverage with C_1 [Eq. (6)].

$$\Theta_1 = \frac{k_{diss}\Theta_{CO}(1-\Theta_{CO})}{k_{diss}\Theta_{CO} + \frac{k_f\Theta_1}{(1-\alpha)}} \quad (6)$$

From this expression we readily find that at a high rate of CO dissociation, $\Theta_1 = 1 - \Theta_{CO}$ and Equation (7).

$$\Theta_{CO} = \sqrt{\frac{k_t}{k_{diss}} k_{ads} P_{CO}} \quad (7)$$

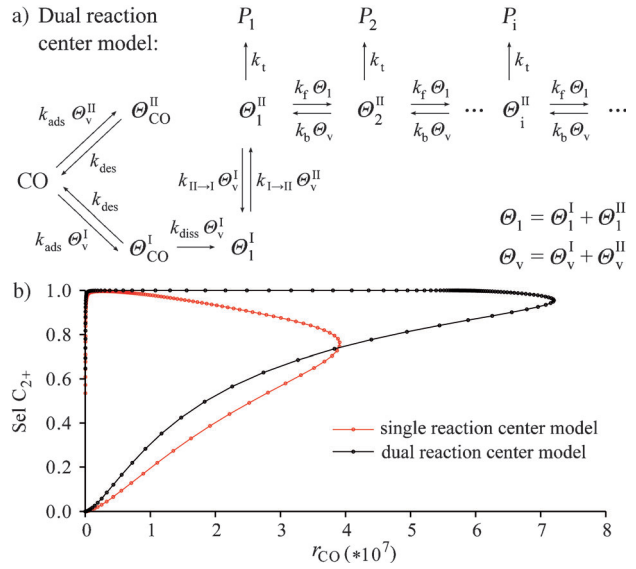

Figure 4. Dual reaction center model for the Fischer–Tropsch reaction. a) CO dissociation only takes place at centers of type I, whereas chain growth only takes place at centers of type II. b) The dual reaction center model, with parameters identical to Figure 3, shows a substantial improvement in the conversion rate for a high selectivity of carbon chains C_{2+} (Sel C_{2+}).

The dissociation of CO is only limited by competitive covering of type I centers with C_1. Higher hydrocarbons grow on the type II centers. The expression for α and the intermediate CO conversion are then given by Equations (8) and (9).

$$\alpha_{dual} = \left(1 + \frac{k_t}{k_f}\frac{1}{1-\Theta_{CO}}\right)^{-1} \quad (8)$$

$$r_{CO} = \frac{k_f^2}{k_t}(1-\Theta_{CO})^3 \quad (9)$$

The linear dependence on the ratio k_t/k_f for α_{dual} implies an increased value compared to the single-center counterpart for the same rate parameters. α_{dual} is found to remain high when the rate of CO dissociation increases and the CO coverage becomes displaced by C_1. The rate of CO consumption remains finite even when k_t becomes small. In this case the CO consumption is controlled by the rate of incorporation of C_1 species into the growing chain. This shows that apart from direct impact on elementary reaction rates, such as the CO dissociation and the cleavage of hydrocarbon chains, the catalyst structure also influences the overall performance more indirectly. Whereas the approximate expressions for a catalyst with single reaction center sites show that the rate of CO consumption to produce C_{2+} is proportional to the fourth root of the product of rates of CH_x insertion into the growing hydrocarbon chain and that of chain termination, and that the reaction rate decreases with increasing CO pressure because of the poisoning of the catalyst with growing chains, the expressions for the dual reaction center model show that the presence of two types of reaction centers may resolve this problem of suppression of CO conversion by the growing hydrocarbon chains. Moreover, these approximate expressions also provide an opportunity to improve macroscopic reactor engineering models that, in analogy to polymerization kinetics, are based on the assumption that C_1 formation is rate controlling.[26]

To conclude, we analyzed the kinetics of the Fischer–Tropsch reaction using a new model that includes reversibility of the chain growth. This model shows that reversibility can be ignored as long as the backward rate is smaller than the forward chain-growth rate. The model also explains the experimentally observed maximum in selectivity for longer chains as a function of the surface reactivity. Moreover, it shows that the surface reactivity for optimal production on a single center site is lower, due to poisoning of the catalyst with growing chains, whereas for a catalyst with sites combining two reaction centers, which might for instance be formed by the addition of promoting reducible oxides, high conversion and selectivity can go hand in hand.

Received: April 28, 2012
Revised: July 10, 2012
Published online: July 24, 2012

Keywords: kinetics · Fischer–Tropsch reaction · heterogeneous catalysis · hydrocarbons

[1] F. Fischer, H. Tropsch, *Brennst.-Chem.* **1926**, *7*, 97.
[2] *Fischer–Tropsch Technology* (Eds.: A. P. Steynberg, M. E. Dry), Elsevier, Amsterdam, **2004**.
[3] H. H. Storch, N. Golumbic, R. B. Anderson, *The Fischer–Tropsch and Related Syntheses*, Wiley, New York, **1951**.
[4] P. Biloen, W. M. H. Sachtler, *Adv. Catal.* **1981**, *30*, 165.
[5] A. T. Bell, *Catal. Rev. Sci. Eng.* **1981**, *23*, 203.
[6] R. A. van Santen, I. M. Ciobica, E. van Steen, M. M. Ghouri, *Adv. Catal.* **2011**, *54*, 127; R. A. van Santen, M. M. Ghouri, S. Shetty, E. J. M. Hensen, *Catal. Sci. Technol.* **2011**, *1*, 891.
[7] J. M. H. Lo, T. Ziegler, *J. Phys. Chem. C* **2007**, *111*, 13149.
[8] J. Chen, Z.-P. Liu, *J. Am. Chem. Soc.* **2008**, *130*, 7929.
[9] Q. Ge, M. Neurock, *J. Phys. Chem. B* **2006**, *110*, 15368.
[10] Q. Ge, M. Neurock, H. A. Wright, N. Srinivasan, *J. Phys. Chem. B* **2002**, *106*, 2826.
[11] J. Cheng, X.-Q. Gong, P. Hu, C. M. Lok, P. Ellis, S. French, *J. Catal.* **2008**, *254*, 285; J. Cheng, T. Song, P. Hu, C. M. Lok, P. Ellis, S. French, *J. Catal.* **2008**, *255*, 20; J. Cheng, P. Hu, P. Ellis, S. French, G. Kelly, C. M. Lok, *J. Phys. Chem. C* **2008**, *112*, 6082.
[12] C.-F. Huo, Y.-W. Li, J. Wang, H. Jiao, *J. Phys. Chem. C* **2008**, *112*, 3840; C.-F. Huo, Y.-W. Li, J. Wang, H. Jiao, *J. Am. Chem. Soc.* **2009**, *131*, 14713; K. F. Tan, J. Xu, J. Chang, A. Borgna, M. Saeys, *J. Catal.* **2010**, *274*, 121; M. Zhuo, K. F. Tan, A. Borgna, M. Saeys, *J. Phys. Chem. C* **2009**, *113*, 8357; T. C. Bromfield, D. C. Ferré, J. W. Niemantsverdriet, *ChemPhysChem* **2005**, *6*, 254; J. Cheng, P. Hu, P. Ellis, S. French, G. Kelly, C. M. Lok, *J. Phys. Chem. C* **2008**, *112*, 6082.
[13] R. A. van Santen, *Acc. Chem. Res.* **2009**, *42*, 57; R. A. van Santen, M. Neurock, S. G. Shetty, *Chem. Rev.* **2010**, *110*, 2005.
[14] I. M. Ciobîcă, G. J. Kramer, Q. Ge, M. Neurock, R. A. van Santen, *J. Catal.* **2002**, *212*, 136.
[15] R. B. Anderson, H. Kölbel, M. Rálekv, *The Fischer–Tropsch synthesis*, Academic Press, Orlando, **1984**.
[16] A. Barbier, A. Tuel, I. Arcon, A. Kodre, G. A. Martin, *J. Catal.* **2001**, *200*, 106; C. G. Visconti, E. Tronconi, L. Lietti, R. Zennaro, P. Forzatti, *Chem. Eng. Sci.* **2007**, *62*, 5338.

[17] A. Logadottir, T. H. Rod, J. K. Norskov, B. Hammer, S. Dahl, C. J. H. Jacobsen, *J. Catal.* **2001**, *197*, 229; V. Pallassana, M. Neurock, *J. Catal.* **2000**, *191*, 301; H. Toulhoat, P. Raybaud, *J. Catal.* **2003**, *216*, 63; R. A. van Santen, M. Neurock, *Molecular Heterogeneous Catalysis*, Wiley, Hoboken, **2006**.

[18] A. J. Markvoort, H. M. M. ten Eikelder, P. A. J. Hilbers, T. F. A. de Greef, E. W. Meijer, *Nat. Commun.* **2011**, *2*, 509; P. A. Korevaar, S. J. George, A. J. Markvoort, M. M. J. Smulders, P. A. J. Hilbers, A. P. H. J. Schenning, T. F. A. de Greef, E. W. Meijer, *Nature* **2012**, *481*, 492; S. Cantekin, H. M. M. ten Eikelder, A. J. Markvoort, M. A. J. Veld, P. A. Korevaar, M. M. Green, A. R. A. Palmans, E. W. Meijer, *Angew. Chem.* **2012**, DOI: 10.1002/ange.201201701; *Angew. Chem. Int. Ed.* **2012**, 10.1002/anie.201201701.

[19] S. G. Shetty, I. M. Ciobica, E. J. M. Hensen, R. A. van Santen, *Chem. Commun.* **2011**, *47*, 9822.

[20] B. Riedmüller, I. M. Ciobica, D. C. Papageorgopoulos, F. Frechard, B. Berenbak, A. W. Kleyn, R. A. van Santen, *J. Chem. Phys.* **2001**, *115*, 5244.

[21] R. M. Watwe, R. D. Cortright, J. K. Norskov, J. A. Dumesic, *J. Phys. Chem. B* **2000**, *104*, 2299.

[22] G. A. Beitel, C. P. M. de Groot, H. Oosterbeek, J. H. Wilson, *J. Phys. Chem. B* **1997**, *101*, 4035.

[23] B. Hammer, J. K. Norskov, *Adv. Catal.* **2000**, *45*, 71.

[24] T. Bligaard, J. K. Norskov in *Chemical bonding at surfaces and interfaces* (Eds.: A. Nilsson, L. G. M. Pettersson, J. K. Norskov), Elsevier, Amsterdam, **2008**, chap. 4.

[25] R. J. Madon, W. F. Taylor, *J. Catal.* **1981**, *69*, 32; L. König, J. Gaube, *Chem. Ing. Tech.* **1983**, *55*, 14; G. A. Huff, C. N. Satterfield, *J. Catal.* **1984**, *85*, 370.

[26] A. Outi, I. Rautavuoma, H. S. van der Baan, *Appl. Catal.* **1981**, *1*, 247; G. Huff, Jr., C. N. Satterfield, *Ind. Eng. Chem. Process Dev.* **1984**, *23*, 696; E. van Steen, H. Schulz, *Appl. Catal. A* **1999**, *186*, 309.

